

# Revolutionizing Nanotechnology with *Filago desertorum* Extracts: Biogenic Synthesis of Silver Nanoparticles Exhibiting Potent Antioxidant and Antibacterial Activities

Published as part of the ACS Omega virtual special issue "Phytochemistry".

Abida Abida, Mikhlid H. Almutairi, Nadia Mushtaq,\* Mushtaq Ahmed, Naila Sher, Fozia Fozia,\* Ijaz Ahmad, Bader O. Almutairi, and Zia Ullah



Cite This: *ACS Omega* 2023, 8, 35140–35151



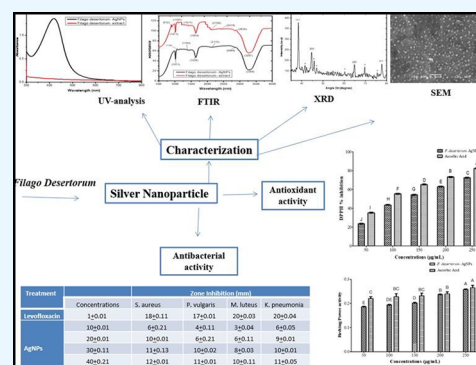
Read Online

ACCESS |

Metrics & More

Article Recommendations

**ABSTRACT:** In this study, we described the environmentally friendly biosynthesis of silver nanoparticles (AgNPs) utilizing ethanolic extract of *Filago desertorum* (*F. desertorum*) as a capping and reducing agent. We also looked at the antioxidant and antibacterial capacities of AgNPs. In order to determine the size, shape, and crystallinity of the created AgNPs, the current project was designed to produce AgNPs utilizing the crude extract of the *F. desertorum*. The effectiveness of the project was evaluated by UV–visible spectrophotometry, Fourier transform infrared spectroscopy, scanning electron microscopy, and X-ray diffraction. AgNPs are monodispersed and spherical and have 50 nm average particle diameters, as determined using Image J software calculations and SEM observation. Four significant peaks from an XRD study, located at 38.46, 44.63, 64.81, and 77.74 nm, were used to calculate the average crystalline size of AgNPs which was reported to be 15 nm. In the crude extract of *F. desertorum*, it is possible to see the functional group peaks of a number of substances that are essential for bioreduction and the stability of the AgNPs. Antibacterial and antioxidant properties of AgNPs in vitro (DPPH, ABTS, H<sub>2</sub>O<sub>2</sub>, phosphomolybdenum, and ferric reducing power) were examined using conventional methods. The AgNPs showed maximum DPPH (72.51% with IC<sub>50</sub> = 144.61  $\mu$ g/mL), ABTS (75.24% with IC<sub>50</sub> = 131.21  $\mu$ g/mL), hydrogen peroxide (73.33% with IC<sub>50</sub> = 115.05  $\mu$ g/mL), phosphomolybdenum activity (73.43% with IC<sub>50</sub> = 75.25  $\mu$ g/mL), and observing reducing power (0.25) at a concentration of 250 g/mL. Inhibition by the AgNPs against the bacterial strain *Staphylococcus aureus* was greatest (12 mm). According to the current findings, AgNPs produced by *F. desertorum* have the highest potential for free radical scavenging and antibacterial activity, which can result in antioxidant and antibiotic agents.



## INTRODUCTION

The creation, manipulation, and application of materials with a range in nanometers constitute the essential scientific topic known as nanotechnology. The name “nano” comes from the Greek word “nanos”, which means dwarf, diminutive, or exceedingly small. Global interest in nanotechnology has considerably increased in recent years. A nanoparticle is a tiny object with a size between 1 and 100 nm. A particle is a small item that functions as a single entity with regard to its attributes and mobility in nanotechnology. Nanoparticles have a wide range of applications in treatments, diagnostics, and medical disciplines. AgNPs have been shown to be the most efficient against bacteria, viruses, and other eukaryotic microbes. Other forms of nanomaterials include copper, zinc, titanium, magnesium, gold, alginate, and silver. Silver nanoparticles (SNPs) created biologically are employed frequently. Water disinfection and the removal of arsenic from water are two

common uses for nanoparticles. Ag nanoparticles are also used in a wide range of other industries, including solar cells and nanoscale detection. For the manufacture of SNPs, green materials such as plant extracts, microbial extracts, algal extracts, and fungal extracts are employed. Silver nanoparticle production is caused by a number of reducing agents found in green extracts. Metal nanoparticles are synthesized using plant extracts. Indeed, due to its quick, nonpathogenic, affordable protocol, and provision of a one-step technique for green synthesis processes, the employment of plants for the assembly of SNPs has drawn a

Received: July 1, 2023

Accepted: September 1, 2023

Published: September 13, 2023



lot of attention.<sup>1</sup> Due to its potential for use in catalysis, biology, computers, solar cells, and optoelectronic devices, such as single electron transistors, nonlinear optical devices, light emitters, drug genes, and photochemical applications, SNPs have received a lot of attention. Antimicrobial SNPs are widely used in the medical field, food preservation, textile coatings, and a variety of environmental applications. SNPs' antimicrobial qualities are advantageous for a variety of industries, including farming, packaging, accessories, cosmetics, health, and the military.<sup>2</sup> The majority of oxidative disorders are brought on by oxidative stress brought on by free radicals. Reactive oxygen species are several types of activated oxygen that include free radicals like superoxide anion, and hydroxyl radicals, and non-radical species like hydrogen peroxide and singlet oxygen (ROS). To balance the output of free themes, one needs a robust antioxidant defense system.<sup>3</sup>

One important etiological element linked to a number of chronic human diseases, including diabetes mellitus, cancer, atherosclerosis, tuberculosis, tetanus, and pneumonia, is the oxidative damage caused by free radical production. Antioxidant therapy has gained significant attention in the discussion of these disorders. Due to their unique electrical, optical, magnetic, chemical, and mechanical properties, metal nanoparticles are currently used in many high-technology fields, including the medical industry for imaging, quicker diagnosis, drug delivery, tissue regeneration, cancer therapeutics, bactericidal and fungicidal agents, and antioxidants, as well as the development of new nanoparticles.<sup>2</sup> A green chemistry strategy for nanoparticle synthesis had to be developed by researchers because the chemical approach of creating nanoparticles was widely used but had potentially harmful effects on the environment.<sup>4</sup> Utilizing bioresources (bacteria, fungi, yeasts, algae, or plants) to create nanoparticles is a very practical, affordable, and environmentally beneficial alternative. AgNPs can be made using less plant-based extract and without the need for additional chemicals or physical processes.<sup>5</sup>

Asteraceae family member *Filago desertorum*, often known as desert cotton roses, is a widespread wild annual desert plant that loves sunny or partly sunny locations and thrives in the sand. "Southern Spain, Afghanistan, Canary Islands, N. Africa, India, M. East, SW Asia, and Pakistan" are all places where this plant is found. *F. desertorum* serves as a source of medicine, grazing, and aromatic compounds. In the current study, we created AgNPs from *F. desertorum* extract and assessed their potential as antioxidants and antimicrobials for biomedical applications.

## MATERIALS AND METHODS

**Chemicals and Instruments.** Silver nitrate ( $\text{AgNO}_3$ , E. Merck, D-6100 Darmstadt, F.R. Germany), Whatman No.1 filter paper, conical flasks, NaOH, pH meter, double beam UV-visible spectrophotometer, Shimadzu spectrophotometer (UV-1800), Shimadzu (IR prestige-21) spectrometer (Japan), potassium bromide (KBr), 1,1-diphenyl-2-picrylhydrazyl (DPPH), 2,2 azobis (ABTS), 3-ethylbenzothiazoline-6-sulfonic acid, ethanol, ascorbic acid, potassium persulfate, sulfuric acid, sodium phosphate, ammonium molybdate, aluminum foil, hydrogen peroxide ( $\text{H}_2\text{O}_2$ ), cork borer, sterile cotton swab, and Levofloxacin were used.

**Plant Collection.** The plant specimens of *F. desertorum* were obtained from the Daryia Kurram region of the Bannu District, close to the village of Ghani Muchen Khel Shahbaz Azmat Khel Bannu. The plant was identified and verified by Professor Dr. Abdur Rehman at the Department of Botany, and the Fd-F-

Ivoucher was deposited. Before being dried in the shade, the plant sample was thoroughly cleaned with tap water and then distilled water. The dried whole plant was ground into a fine powder using an electric grinder and stored for later use in an airtight container.

**Plant Extract Preparation.** About 10 grams of whole plant powder was weighed out to create the extract, which was then steeped for 24 h in 100 mL of ethanol. The liquid was put into a conical flask and gently centrifuged at 6000 rpm for 30 min after being filtered through no. 1 filter paper (rpm). The supernatant was taken out for usage after 30 min of centrifugation, and the pellet was discarded (Goodarzi et al.).

**Silver Nanoparticle Green Synthesis Methodology.** For the green synthesis of AgNPs, the plant extract was diluted five times and combined with  $\text{AgNO}_3$  (4 mM) solution. 98% NaOH was used to alter the pH to 9 (3 mM). *F. desertorum* plant supernatants were diluted five times (20 mL extract + 80 mL deionized water + NaOH) and mixed with a silver nitrate solution at 35 °C (5 mL). The color of the resulting solution changes from yellowish to dark brown after 10 min at 350 °C temperature. This coloring suggested the creation of AgNPs. Using a UV-visible spectrophotometer, the solution was checked after 24 h of complete stabilization. It was then centrifuged in a cold centrifuge at 4 °C and 13,000 rpm for 10 min; after centrifugation, the supernatants were discarded and the pellet was kept. The pellet was collected, suspended in sterile double distilled water, and lyophilized for freeze-drying.<sup>6</sup>

**Influencing Variables for the Formation of AgNPs.** *Effect of Variation of Temperature.* AgNPs were created in the current experiment at temperatures ranging from 20, 25, 30, and 35 °C. The UV spectra of each aqueous suspension were measured.

*Effect of Variation of pH.* Using 0.2 M NaOH and 0.2 M HCl, the current study investigated the effects of acidic and basic conditions on the synthesis of AgNPs at various pH values of 3–12, respectively. Afterward, each aqueous suspension's UV spectra were identified.

*Effect of Incubation Time.* After 5 min of synthesis, the temporal impact on AgNPs synthesis was examined, and 24 h later, the ultimate reaction was noticed. The absorbance was calculated using a UV-visible spectrophotometer.

*Effect of Variation of Plant Extract Concentration.* In the current study, the impact of plant extract concentration on the synthesis of AgNPs was studied at various ranges (1.2–2 mL). The absorbance was calculated using a UV-visible spectrophotometer.

*Effect of Variation of  $\text{AgNO}_3$  Concentration.* In the current study, several  $\text{AgNO}_3$  concentration ranges were studied for their impact on AgNP generation (0.5–4 mM).

**Green Synthesized AgNP Characterization.** *Analysis Using a UV-Visible Spectrophotometer.* It was feasible to ascertain the stability and production of AgNPs (the reduction of silver ions ( $\text{Ag}^+$ )) with a double-beam UV-visible spectrophotometer and the Shimadzu UV-spectrophotometer (UV-1800), at wavelengths between 200 and 800 nm.

*Analysis Using a Fourier Transform Infrared (FTIR) Spectrometer.* Using FTIR measurement with a Shimadzu (IR prestige21) spectrometer, the peaks for the different functional groups were found (Japan). The created samples of each extract and AgNPs were completely dried to remove even the smallest amount of moisture before being subjected to FTIR analysis. The potassium bromide (KBr) powder was similarly dried two to three times in the sample before FTIR analysis. A pure

potassium bromide pellet was used for the blank analysis. Thin pellets containing about 5% of each sample were created as the potassium bromide solid solution for each sample.

**Analysis by Scanning Electron Microscopy (SEM).** Using a JEOL SEM Model JSM5910, the shape, sizes, and dispersion of AgNPs discovered on the surface have been examined (Japan). The current–voltage of the project ranged from 5 to 20 kV, and the microscopic lens's resolution was 10,000X to 50,000X. The necessary amount of AgNPs was placed on aluminum stubs with conductive taps before being exposed to SEM analysis.

The average AgNP particle size was determined from SEM resolution using Image J software.

**Analysis Using X-ray Diffraction (XRD).** The structure of the AgNPs was established using the JDX3532 (JEOL JAPAN) XRD with set 1.54 Å radiation wavelengths. Each specimen was around one square meter in length for XRD examination. The specimen was then placed in a glassy handle for transfer into the X-ray generating duct. The scanner degrees were set to 50°, and a current of 20 mA (milli ampere) and 35 kV (kilo volt) of speed-up voltage were supplied. There were measurements of light intensities between 20° and 80°, utilizing the Debye–Scherrer equation. To determine the average crystal size, utilizing the Debye–Scherrer equation,

$$D = k\lambda/\beta\cos\theta$$

**In Vitro Antioxidant Assays. 1,1-Diphenyl-2-picrylhydrazyl (DPPH) Radical Scavenging Activity.** The DPPH free radical inhibition activity was carried out using the Brand-Williams protocol.<sup>7</sup> The stock solution was made by dissolving 3 mg of DPPH in 100 mL of ethanol, and the mixture was then maintained at 25 °C. The solution was further diluted with ethanol and measured using a spectrophotometer to produce an absorbance at 517 nm. Separately, 5 mg of AgNPs and 5 mg of ascorbic acid were dissolved in 5 mL of deionized water. Pipette 50 mL of the stock solution (5 mg/5 mL) and combine it with 950 mL of ethanol/deionized water to create 50 g/mL concentrations. Likewise, for g/mL values of 50, 100, 150, 200, and 250, ethanolic DPPH solution was used as a control. The absorbance of a test tube containing 200 mL of *F. desertorum* AgNPs at various concentrations (50–250 g/mL), and 2 mL of DPPH solution was measured using a spectrophotometer at 517 nm after 20 min of room temperature and darkness (SP300 Japan). The experiment was done in triplicate, and ascorbic acid was utilized as the standard. The % inhibition was calculated using the equation shown below.

Scavenging (percentage) inhibition

$$= [(control - test sample)/(control)] \times 100$$

**ABTS (2,2 Azobis, 3-Ethylbenzothiazoline-6-sulfonic Acid) Radical Scavenging.** ABTS inhibitory activity was assessed using the Brand-Williams protocol.<sup>7</sup> ABTS (7 mM) was mixed with potassium persulfate solution (2.45 mM) and left to remain in the dark for 24 h to create the ABTS solution. A spectrophotometer was used to further dilute the ABTS solution with water to generate an absorbance (1 and >0.4) at 745 nm. Separately, 5 mg of AgNPs and 5 mL of ascorbic acid stock solution were dissolved in 5 mL of deionized water to provide concentrations of 50, 100, 150, 200, and 250 g/mL. The capacity of ABTS to inhibit was determined by combining 200 L of AgNPs with 2 L of ABTS solution in test tubes and incubating for 6 min. After 6 min, the absorbance at 745 nm was measured.

The experiment was carried out three times. The % inhibition was calculated using the equation shown below:

Scavenging (percentage) inhibition

$$= [(control - test sample)/(control)] \times 100$$

**Phosphomolybdate Assay (PMA).** Different concentrations of 50, 100, 150, 200, and 250 g/mL of ascorbic acid and AgNPs were used in PMA via modified method of Brand-Williams.<sup>7</sup> In a nutshell, 0.1 mL of various AgNP concentrations (ranging from 50 to 250 g/mL) were combined with 1 mL of phosphomolybdate reagent solution (0.6 M sulfuric acid, 28 mM sodium phosphate, and 4 mM ammonium molybdate) in a test tube. After that, aluminum foil was used to seal the test tube, which was then heated to 95 °C. The absorbance of the combination at 765 nm was calculated in comparison to a blank. The standard used was ascorbic acid. Three separate runs of the assay were made (Umamaheswari and Chatterjee, 2008). The % inhibition was calculated using the equation shown below.

Scavenging (percentage) inhibition

$$= [(control - test sample)/(control)] \times 100$$

**Hydrogen Peroxide (H<sub>2</sub>O<sub>2</sub>) Scavenging Assay.** Phosphate buffer was used to prepare a 50 mM H<sub>2</sub>O<sub>2</sub> solution (50 mM, pH 7.4). Separately, 5 mg of AgNPs and 5 mL of ascorbic acid stock solution were dissolved in deionized water to provide concentrations of 50, 100, 150, 200, and 250 g/mL. In a test tube with a silver foil top, 0.6 mL of hydrogen peroxide solution was combined with 1.5 mL of AgNPs solution at various concentrations, and the mixture was incubated for 15 min. The absorbance of 230 nm was assessed upon incubation and compared to a control solution. Ascorbic acid was used as the reference. The experiment was carried out. The experiment was carried out three times by Brand-Williams.<sup>7</sup> The following equation was used to calculate the % inhibition.

Scavenging (percentage) inhibition

$$= [(control - test sample)/(control)] \times 100$$

**Reducing Power Assay.** Separately dissolving 5 mg of AgNPs and 5 mg of ascorbic acid in 5 mL of deionized water produced concentrations of 50, 100, 150, 200, and 250 g/mL. 500 L of potassium ferricyanide (10 mg/L), 500 L of phosphate buffer (0.2 M, pH 6.6), 500 L of AgNPs from concentrations of 50–250 g/L, and 500 L of trichloroacetic acid (0.1 g/L) were combined and incubated at 60 °C for 30 min in a water bath. A tube containing 1 mL of the aforementioned solution, 1 mL of distilled water, and 0.2 mL of 0.1% (w/v) ferric chloride was incubated for 15 min. The reaction's absorbance was measured at 700 nm after 15 min Brand-Williams et al.<sup>7</sup> The experiment was run three times.

**In Vitro Antibacterial Assay.** *F. desertorum* AgNPs was evaluated using agar well diffusion method of Ruparella et al.,<sup>8</sup> with certain adjustments for use against *Klebsiella pneumoniae*, *Proteus vulgaris*, *Micrococcus luteus*, and *Staphylococcus aureus*. For the nutritious, aseptic agar plates, a 24-h incubation period was used. To establish a bacterial lawn, a 24-h culture from the nutrient broth was applied to the sterile nutrient agar plates using a sterile cotton swab. Each plate has five wells created with a sterile 6 mm cork borer. AgNPs (10, 20, 30, and 40 mg/mL) were added in varying concentrations to each well, along with 100 L of a Levofloxacin (reference medication) solution, which

was then incubated at 37 °C for 24 h. The inhibition zone was measured in mm after 24 h in contrast to the reference medication (positive control).

**Statistical Analysis.** All data are expressed as mean  $\pm$  S.D. Graphs were analyzed by OriginPro, 2018 and slideWrite software. Statistical analyses were performed using two-way ANOVA with drug treatment and dose as independent variables and conducted with Bonferroni post-tests to examine the differences between the different drug treatment regimens and the diverse responses. A  $p$  value of 0.05 was considered statistically significant.

## RESULTS

**Biosynthesis of AgNPs.** In 10 min, the color of a 2 mL extract of *F. desertorum* added to a 4 mM solution of AgNO<sub>3</sub> at pH 9 changed from colorless to yellowish-dark brown. After 24 h, the final coloration emerged (Figure 1). Crude plant extracts reduce the silver ion, resulting in the formation of AgNPs.

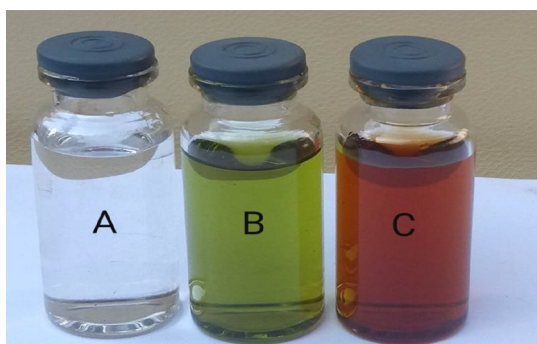


**Figure 1.** Visual analysis of the color change of *F. desertorum* in AgNPs (A) AgNO<sub>3</sub> solution, (B) *F. desertorum* extract, and (C) biosynthesized AgNPs.

**UV–Visible Analysis.** Figure 2 shows the UV–vis spectroscopy results from the interaction of an extract of *F. desertorum* with a water-soluble solution of AgNO<sub>3</sub>. As the plant extract solution was added, the color of the silver salt started to change, signifying the creation of AgNPs. The

production of AgNPs in the liquid phase was demonstrated using UV–visible spectroscopy. The absorbance peak of the AgNPs is at 420 nm (1.3572).

**Factors Effecting on Synthesis of AgNPs. Temperature Effect.** The creation of AgNPs is significantly influenced by temperature. According to the results shown in Figure 3, the absorption spectra curve for *F. desertorum* was measured by a UV–visible spectrophotometer at 404 nm (0.24) at 20 °C, 403 nm (0.32) at 25 °C, 401 nm (0.42) at 30 °C, and 420 nm (1.35) at 35 °C, respectively.

**Effect of Variation of pH.** AgNPs have been produced at a variety of pH levels, including 3–12. The pH has been cited as a significant factor in this process. The effect of pH on the reduction of Ag<sup>+</sup> ions is depicted in Figure 4. At pH 3–5, there was no reaction, while at pH 6–12, AgNPs were produced. At pH 9, the maximum peak was attained.

**Effect of Variation of Incubation Time.** After 10 min, each liquid suspension in the current investigation displayed broad bands. The band began sharpening and displaying the presence of AgNPs after 30 min. The continual generation of AgNPs during the reaction process led to a rapid increase in absorption band intensity when the incubation duration was increased from 5 min to 24 h. For *F. desertorum*, the absorption bands were 418 nm (0.51) at 5 min, 428 nm (0.67) at 10 min, 427 nm (0.69) at 30 min, 427 nm (0.72) at 1 h, and 420 nm (1.35) at 24 h (Figure 5).

**Effect of Variation of Each Plant Extract Concentrations.** The quantity of plant materials is one of the crucial elements that affect the characteristics of nanoparticles. At varied extracts of 1.2, 1.4, 1.6, 1.8, and 2 mL, the green color's apparent absorption peak formed by AgNPs with a wavelength range of 300–800 nm is shown in Figure 6. It has been discovered that when extract concentration rises, the absorbance band's intensity rises. The extract concentration in 2 mL displayed a 420-degree acute absorption peak.

**Effect of Variation of AgNO<sub>3</sub> Concentrations.** The observed absorbance values of green AgNPs at different AgNO<sub>3</sub> concentrations of 0.5, 1, 2, 3, and 4 mM are shown in Figure 7. It has been discovered that when the concentration of AgNO<sub>3</sub> increases, the intensity of the absorbance peak also increases.

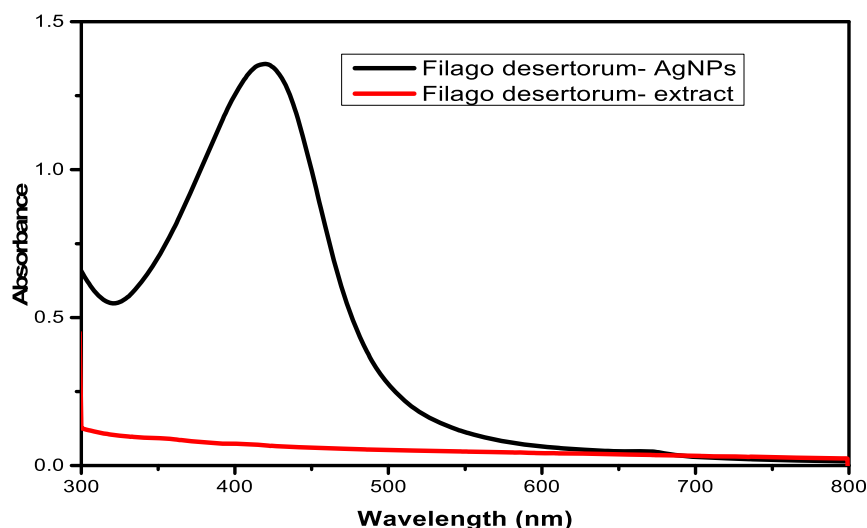


**Figure 2.** AgNPs' UV–visible absorption spectra. Volume: 2 mL, duration: 24 h, temperature: 35 °C, AgNO<sub>3</sub> concentrations: 4 mM, and pH: 9 were used to study *F. desertorum*.

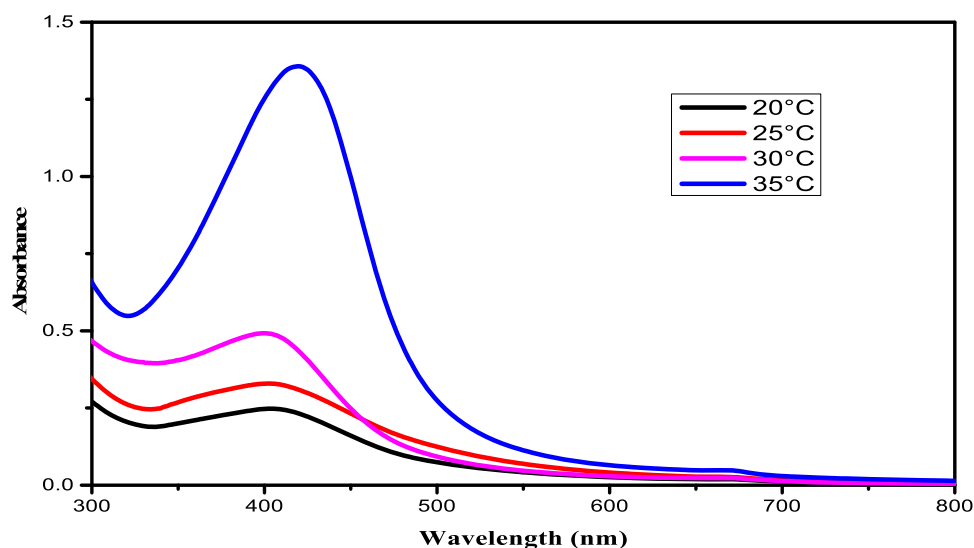


**Figure 3.** Temperature-dependent UV–visible absorption spectrum of AgNPs. 2 mL of *F. desertorum* extract, 4 mM of AgNO<sub>3</sub>, 24 h, and a pH of 9 were used.

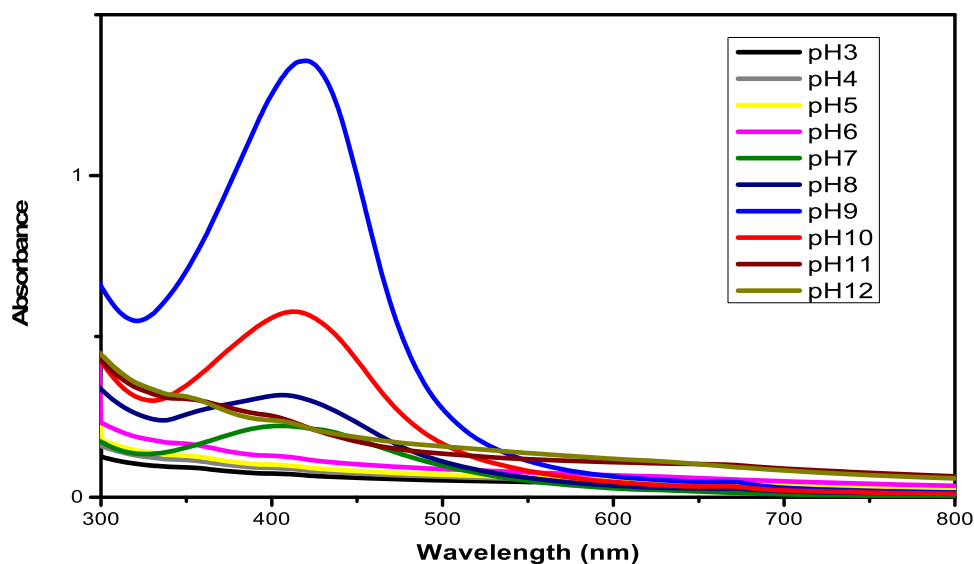


**Figure 4.** AgNPs' UV–vis absorption spectrum in neutral, acidic, and basic conditions. 2 mL, 4 mM AgNO<sub>3</sub> concentration, 35 °C, and 24 h were used to study *F. desertorum*.

The AgNO<sub>3</sub> concentration at 4 mM produced a 420 nm absorbance peak.

#### Analysis through FTIR Spectrometry

Using FTIR analysis, the correct compounds that are present in the extract and are in charge of reducing silver ions were found. A variety of bands related to various functional groups that are actively involved in the bio reduction of Ag ions and act as reducing agents can be seen in the findings of an FTIR spectrum. By comparing the recorded FTIR bands to reference bands in the FTIR chart, it was possible to identify the precise functional groups involved in the reduction process. Bands at 3287, 2834, 2421, 2108, 1654, 1411, 1107, and 1011 cm<sup>-1</sup> are present in the *F. desertorum* AgNPs (Figure 8).

**Analysis through SEM.** The form and diameter of the biosynthesized AgNPs were measured using SEM. The circular shape and uniform dispersion of the biosynthesized AgNPs in the nanoparticles are shown in the micrograph images (Figure 9a). Using By means of SEM examination and usage of

NaoMeasure software, the size of the Biosynthesized AgNPs in the nanoparticles were determined and the calculated size was reported to be 50-nm by marking 15 particles in the SEM images (Figure 9b).

**Analysis through XRD.** The XRD pattern analysis of the produced AgNPs is shown in Figure 10. Four distinct bands at 38.46°, 44.63°, 64.81°, and 77.74°, respectively, displayed the Ag ion representations (111), (200), (220), and (311). For *F. desertorum*, the (111) reflection could be visualized as a distinct and crisp XRD peak that was discovered at 38.46°, which was exactly in agreement with the Joint Committee on Power Diffraction Standards' standard reference values (JCPDS no. 893722). AgNPs' average crystalline size, as determined by the Debye–Scherrer equation, was determined to be 15 nm. Table 1 shows the measured interplaner spacing (dhkl) at d111, d200, d220, and d311 as well as the Miller constants (a0) of SNPs.

**In Vitro Antioxidant Assays of AgNPs. DPPH Assay.** The DPPH radical scavenging activity of ascorbic acid and AgNPs at

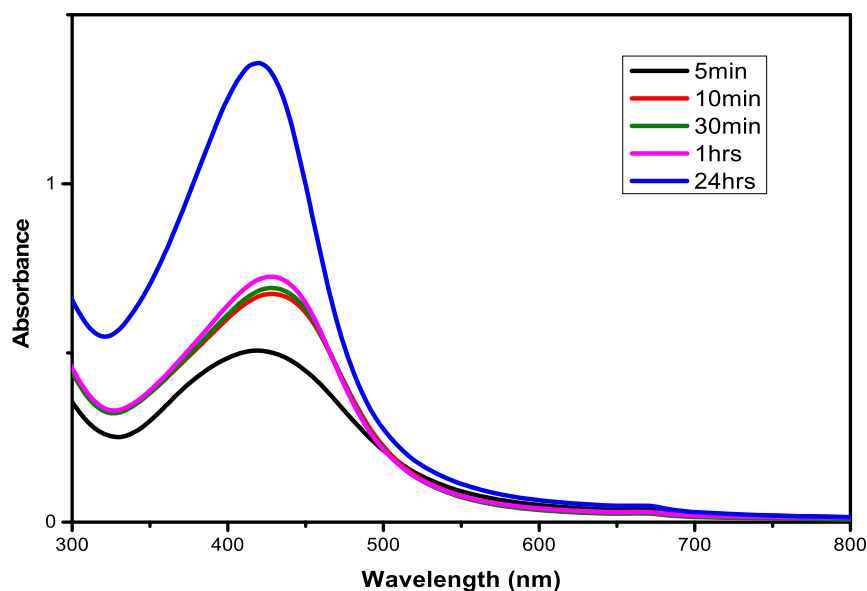


**Figure 5.** AgNPs' UV-vis absorption spectrum at various time intervals. 2 mL, 35 °C, 4 mM AgNO<sub>3</sub> concentration, and pH 9 were used to study *F. desertorum*.

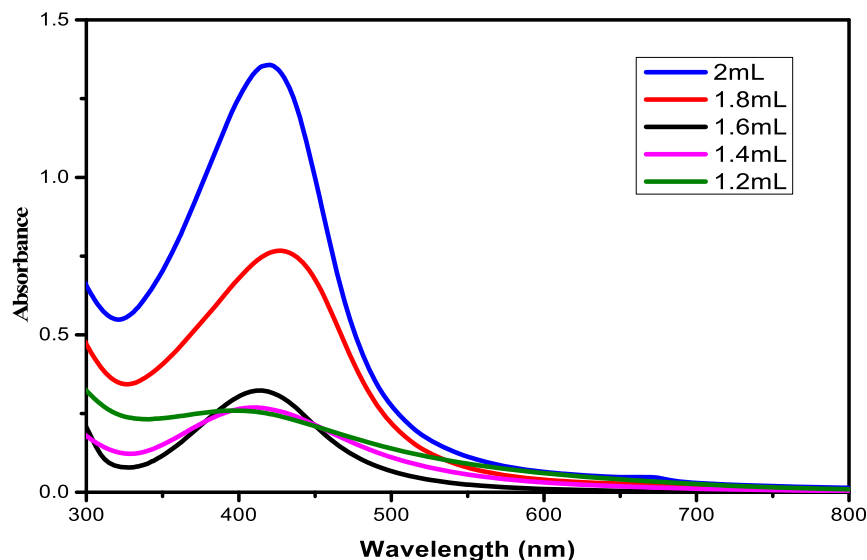


**Figure 6.** UV-vis absorption spectra with various concentrations of *F. desertorum* extract throughout the course of a 24-h period at a temperature of 35 °C and a pH of -9.

various doses is shown in Figure 11. AgNPs' IC<sub>50</sub> value was determined to be 144.61 ± 0.22 μg/mL. Maximum DPPH radical scavenging activity was attained at doses of 250 μg/mL for both AgNPs and standard ascorbic acid 82.34 ± 0.34 and 68 ± 0.24%, respectively. The testing samples were effective at scavenging radicals in a concentration-dependent way. The IC<sub>50</sub> value for the reference medication, ascorbic acid, was at 95.29 ± 0.11 μg/mL. Ascorbic acid is statistically different from the AgNPs.

**ABTS Radical Scavenging Assay of AgNPs.** The highest levels of ABTS radical scavenging activity were seen in SNPs and ascorbic acid (standard) (Figure 12). The AgNPs from *F. desertorum* had the greatest inhibitory effect on the ABTS radicals at a concentration of 250 μg/mL. The IC<sub>50</sub> values of AgNPs is 131.21 ± 0.22 μg/mL and ascorbic acid is 97.35 ± 0.23 μg/mL. Ascorbic acid is statistically different from the AgNPs.

**PMA of AgNPs.** With the help of SNPs and ascorbic acid, molybdenum (VI) is changed to molybdenum (V), creating the green chemical phosphomolybdenum V. The overall antioxidant capacity of different quantities of ascorbic acid and SNPs from *F. desertorum* is shown in Figure 13. Ascorbic acid and AgNPs from *F. desertorum* had IC<sub>50</sub> values of 75.25 ± 0.23 and 52.82 ± 0.11 μg/mL, respectively (Table 2). The results show that although the reference antioxidant (ascorbic acid) had more antioxidant properties than the 250 μg/mL AgNPs, ascorbic acid is statistically different from the AgNPs.

**Hydrogen Peroxide (H<sub>2</sub>O<sub>2</sub>) Scavenging Assay of AgNPs.** AgNPs (73.33 ± 0.22%) and ascorbic acid (85.55 ± 0.11%) had their highest scavenging action at a higher concentration (250 μg/mL) (Figure 14). AgNPs and ascorbic acid both had IC<sub>50</sub> values of 115.05 ± 0.11 and 87.93 ± 0.11 μg/mL, respectively (Table 2). According to the IC<sub>50</sub> value, the AgNPs have a strong hydrogen peroxide scavenging capacity but less than ascorbic

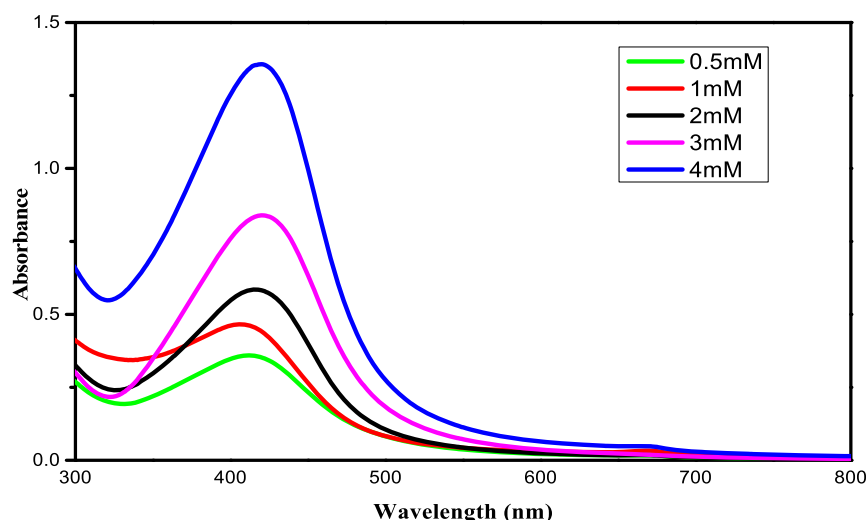


**Figure 7.** UV–visible absorption spectra at various  $\text{AgNO}_3$  concentrations, *F. desertorum* extract volume of 2 mL, time of 24 h, temperature of 35 °C, and pH of –9.

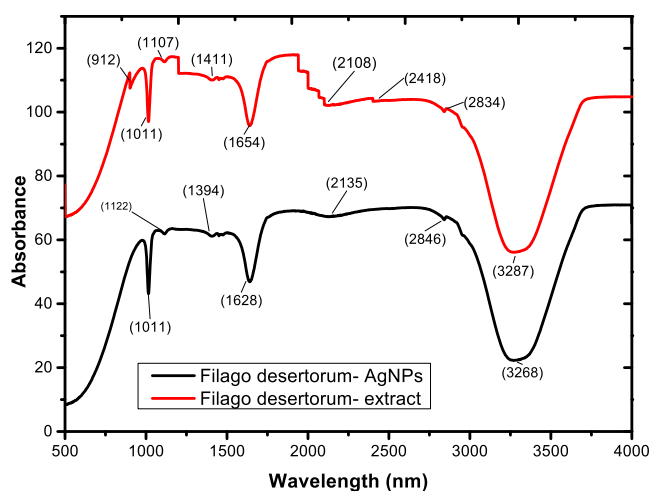
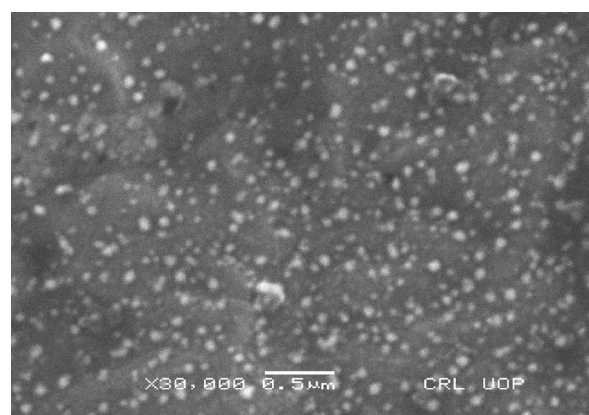


**Figure 8.** FTIR spectroscopy of plant extract and AgNPs.

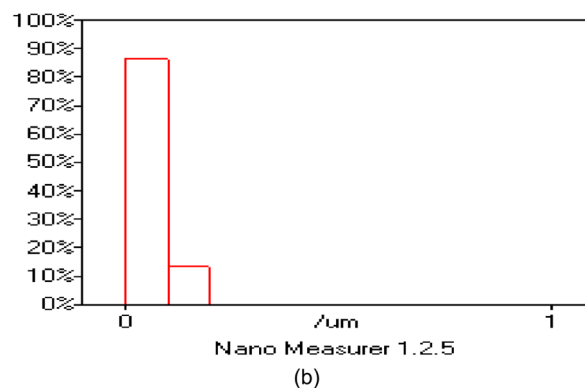
acid. In our analysis, the  $\text{H}_2\text{O}_2$  radical scavenging increased along with the sample material amount. Ascorbic acid is statistically differed from the AgNPs.

**Reducing Power Assay of AgNPs.** Figure 15 shows the ascorbic acid and *F. desertorum* AgNPs' lowering abilities. The reducing power of ascorbic acid and AgNPs increases as their concentrations do. Comparatively to other concentrations, the 250  $\mu\text{g}/\text{mL}$  concentration had the greatest lowering power effect. The AgNPs (0.25 + 0.21) observed strong reducing power abilities, which were reduced when compared to ascorbic acid, in a concentration-dependent way (0.26 + 0.31). Increases in reducing ability are correlated with increases in absorbance. Ascorbic acid is statistically differed from the AgNPs.

**Antibacterial Activity of AgNPs.** The results of this investigation show that SNPs from *F. desertorum*, at concentrations of 10–40  $\text{mg}/\text{mL}$ , showed good antibacterial activity against both Gram-positive (*S. aureus* and *M. luteus*) and Gram-negative (*Klebsiella pneumoniae* and *P. vulgaris*) bacteria (Table 3). AgNPs' inhibitory zones ranged in size from 3 to 12 mm. *S. aureus* had the largest zone of inhibition (12 mm) for AgNPs, whereas *M. luteus* demonstrated the smallest zone of inhibition (10 mm). Levofloxacin's inhibitory zones ranged from 17 to 20 mm (Figure 16).



(a)



(b)

**Figure 9.** (a) Scanning electron microscopy of AgNPs. (b) Nano-Measurer calculated size of AgNPs.

## DISCUSSION

The current study generated AgNPs using the crude extract of *F. desertorum*. Using UV–vis, AgNPs in aqueous solutions were identified.<sup>5</sup> Our results concurred with those of Sher et al.,<sup>9</sup> who recorded the AgNPs' peak at 415 nm. The investigation of our findings is also supportive of Hernandez-Gomora et al.<sup>10</sup> that the AgNPs exhibit characteristic absorbance at about 430 nm.

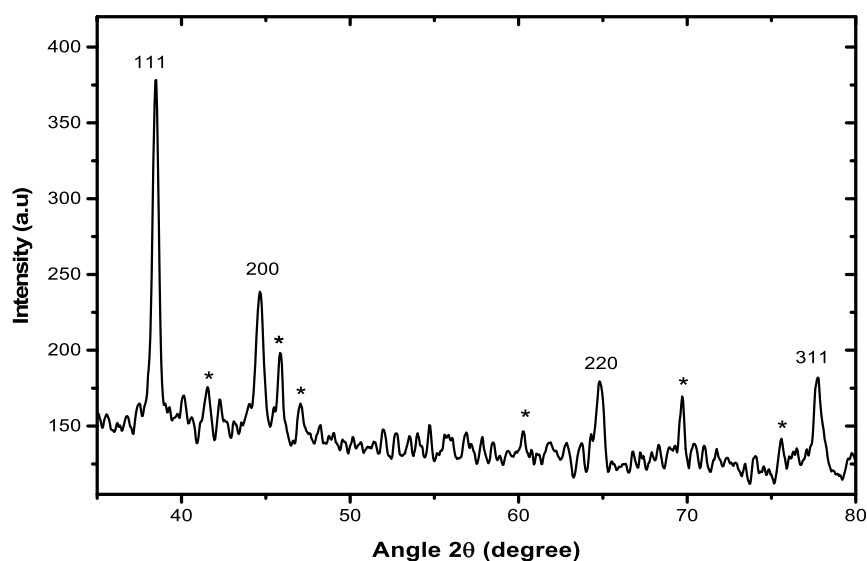


Figure 10. X-ray diffraction analysis of AgNPs.

Table 1. Using the Scherrer Equation and XRD, the Average Particle Size, Interplanar Spacing, and Lattice Constant of AgNPs Were Determined

angle ( $2\theta$ )	interplanar spacing	full width at half-maximum	Miller constants ( $\text{\AA}$ )	size (nm)
38.463°	111	0.43	4.05	18
44.635°	200	0.57	4.05	13
64.815°	220	0.40	4.06	17
77.748°	311	0.52	4.07	12

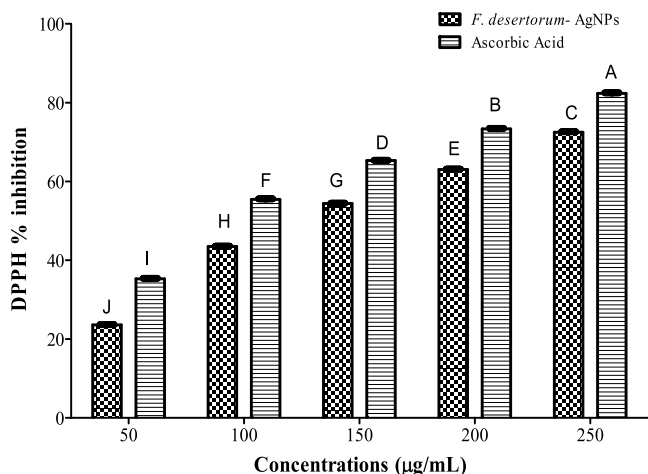


Figure 11. AgNPs and ascorbic acid have DPPH scavenging action (Figure 11). The values are displayed as mean SD ( $n = 3$ ). Means with various letters display the important variations. A one-way analysis of variance (ANOVA) was used to compare the data, and then the least significant differential test (LSD = 0.20) was performed with a 5% significance threshold ( $P < 0.05$ ).

Researchers discover that as temperature rises, AgNP synthesis rates rise as well. The average size of AgNPs is said to be reduced by increasing the surface plasmon resonance band's intensity, which is induced by raising the temperature.<sup>11</sup> AgNP synthesis required an optimum condition for their synthesis; in order to obtain small size AgNPs, different factors were followed in the current study, i.e., different pH, temperature, plant extract concentration, and Ag salt concentration. The 35 °C temper-

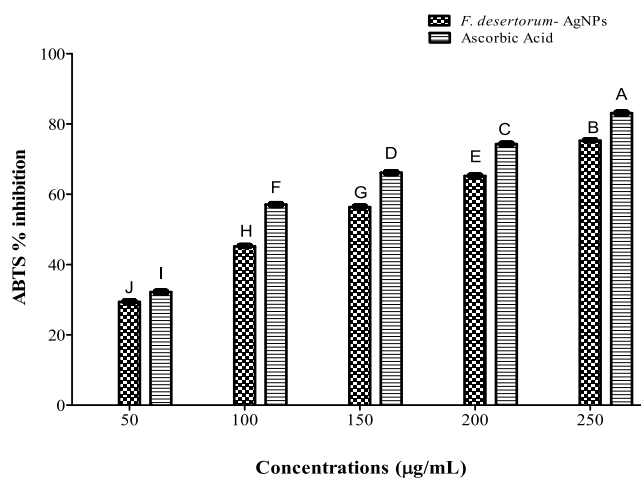
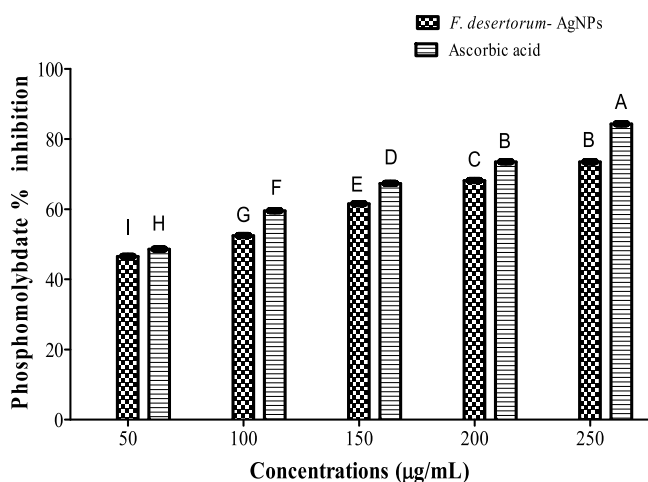


Figure 12. AgNPs and ascorbic acid's ability to scavenge ABTS. The values are displayed as mean SD ( $n = 3$ ). Means with various letters display the important variations. The least significant difference (LSD = 0.23) test was used to compare the data after a one-way analysis of variance (ANOVA) at a significant threshold of 5% ( $P < 0.05$ ).

ature provided a satisfactory peak in the current investigation. At a temperature of 35 °C, the bioactive components of *F. desertorum* may be gradually decreased and stabilized as AgNPs. A free NPs, as many theoretical models assume, has a different melting temperature (usually lower) than a supported particle due to the absence of cohesive energy between the NPs and substrate. The current findings are consistent with those of Hernandez-Gomora et al.,<sup>10</sup> who used *Azadirachta indica* aqueous leaf extract to make environmentally friendly AgNPs and who verified that silver ions must be heated to 23 °C in order to become AgNPs. The pH has been shown to be one of the main markers in AgNP syntheses and is an important element in the formation of AgNPs. There was observable AgNP synthesis when the pH of a sample was changed from acidic to alkaline. Since nanoparticles disintegrate in acidic environments, the absence of nanoparticle production in the sample was caused by the presence of smooth absorption bands at pH 3–5.<sup>12</sup> At pH 9, it was noted that there were sharp peaks at 420 nm and the outcome of Sher et al.<sup>2</sup> In the current work, an acceptable



**Figure 13.** AgNPs and ascorbic acid's phosphomolybdate (PMA) activity. The values are displayed as mean SD ( $n = 3$ ). Means with various letter combinations show significant variations, whereas means with identical letter combinations show non-significant differences. The least significant differential test (LSD = 0.08) was used to compare the data after a one-way analysis of variance (ANOVA) at a significant threshold of 5% ( $P < 0.05$ ).

**Table 2.** IC<sub>50</sub> Values of Antioxidant Activities of AgNPs and Ascorbic Acid

parameters	<i>F. desertorum</i> AgNPs (µg/mL)	ascorbic acid (µg/mL)
DPPH scavenging assay	144.61 ± 0.22	95.29 ± 0.11
ABTS scavenging assay	131.21 ± 0.22	97.35 ± 0.23
phosphomolybdate assay	75.25 ± 0.23	52.82 ± 0.11
H <sub>2</sub> O <sub>2</sub> scavenging assay	115.05 ± 0.11	87.93 ± 0.11

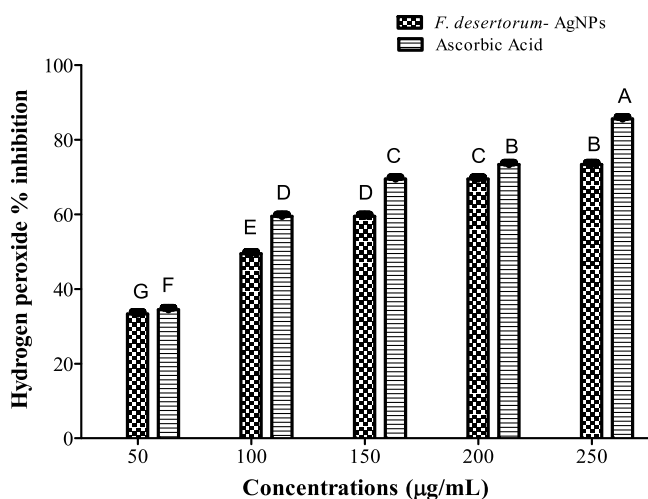


**Figure 14.** AgNPs and ascorbic acid's ability to scavenge H<sub>2</sub>O<sub>2</sub>. The values are displayed as mean SD ( $n = 3$ ). Means with various letter combinations show significant variations, whereas means with identical letter combinations show non-significant differences. The least significant differential (LSD = 0.94) test was used to compare the data after a one-way analysis of variance (ANOVA) at a significant threshold of 5% ( $P < 0.05$ ).

alkaline setting for AgNP production was reported to be pH 9. The absorbance decreased at pH 11 and 12, indicating aggregation of the nanoparticles. Small AgNPs are formed when the nucleation process dominates the aggregation process

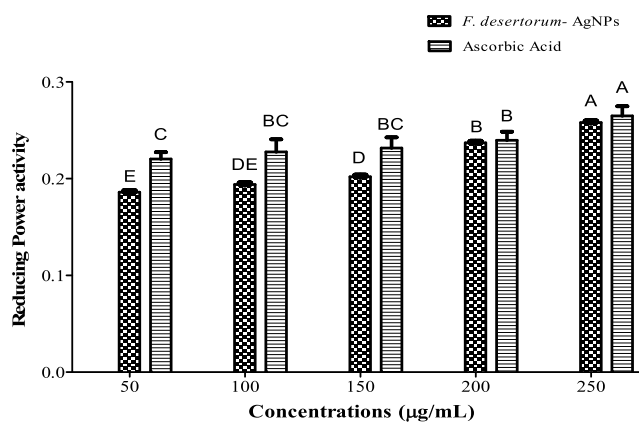


**Figure 15.** AgNPs and ascorbic acid's reducing power activity. Data are shown as mean standard deviation (triplicates test). Means with various letter combinations show significant variations, whereas means with identical letter combinations show non-significant differences. The least significant differential test (LSD = 0.01) was used to compare the data after a one-way analysis of variance (ANOVA) at a significant threshold of 5% ( $P < 0.05$ ).

in alkaline solutions as opposed to acidic solutions where the nucleation process dominates.<sup>13</sup> Our findings agree with those of Sher et al.,<sup>2</sup> and they claimed that a pH of 9 was more suited for the production of AgNPs. At 5, 10, 30, and 60 min at room temperature, the reaction between the plant extract and silver nitrate is constantly recorded, producing different peaks at different times. After the *F. desertorum* extracts and silver nitrate solution reacted for 10 min, a color shift from green to brown was visible. The color darkened over time to become brown.<sup>14</sup> After 10 min of exposure, the surface plasmon resonance (SPR) band widens as a result of the gradual conversion of silver ion (Ag<sup>+</sup>) to zero valent silver (Ag<sup>0</sup>) NPs. When the response time increased, a good peak in surface plasmon resonance was seen because more Ag<sup>+</sup> had been transformed to Ag<sup>0</sup>. After 24 h, the major surface plasmon resonance band for AgNPs was discovered at 420 nm. Findings from the literature indicate that when the color is persistent and the SPR has a sharp peak, the necessary duration is attained. In the study conducted by Ramkumar et al.,<sup>15</sup> AgNPs started to develop after just 30 min of incubation and it was found. The number of biomaterials in the extract affects how many metallic nanoparticles are created. Two milliliters of *F. desertorum* sample was said to contain the sharp peak.

Our results are corroborated by those of Kumar et al.,<sup>16</sup> who created environmentally friendly AgNPs using various amounts of *Prunus persica* plant extract (1–5 mL). Our findings were significantly corroborated by the produced AgNPs employing 2 mL of *Matricaria recutita* (Babunah) extract. The amount of silver nitrate present has a big impact on how AgNPs develop. In this study, the optimal Ag ion concentration for manufacturing Ag nanomaterial was identified. In the present study, the 420 nm strong peak was observed at the optimum AgNO<sub>3</sub> concentration of 4 mM. According to a number of studies, the amount of silver nitrate used in the synthesis process can influence the creation of AgNPs. Our results support those of Hazarika et al.,<sup>17</sup> who noticed that employing *O. tenuiflorum* extract as a reductant, and 4 mM concentration of silver nitrate solution created a strong peak of SNPs and that the absorption spectra of AgNPs increased with silver salt concentration (1–5 mM). *F. desertorum* extract and AgNPs underwent FTIR analysis to identify the active chemicals present. The greatest absorption

Table 3. Antibacterial Activity of *F. desertorum* AgNPs

treatment	concentrations (mg/mL)	zone inhibition (mm)			
		<i>S. aureus</i> (ATCC 29213)	<i>P. vulgaris</i> (ATCC 4111)	<i>M. luteus</i> (ATCC 4698)	<i>K. pneumoniae</i> (ATCC 700603)
Levofloxacin (+control)	1 ± 0.01	18 ± 0.11	17 ± 0.01	20 ± 0.03	20 ± 0.04
<i>F. desertorum</i> AgNPs	10 ± 0.01	6 ± 0.21	4 ± 0.11	3 ± 0.04	6 ± 0.05
	20 ± 0.01	10 ± 0.01	6 ± 0.21	6 ± 0.11	9 ± 0.01
	30 ± 0.11	11 ± 0.13	10 ± 0.02	8 ± 0.03	10 ± 0.01
	40 ± 0.21	12 ± 0.01	11 ± 0.01	10 ± 0.11	11 ± 0.05

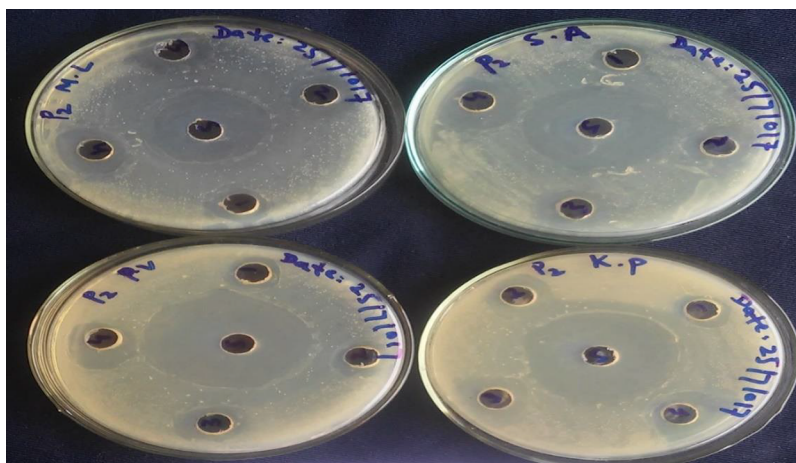


**Figure 16.** Antibacterial efficacy of *F. desertorum* AgNPs against both Gram-positive (*S. aureus* and *M. luteus*) and Gram-negative bacteria (*Klebsiella pneumoniae* and *P. vulgaris*).

peaks for the AgNPs and the *F. desertorum* extract were 1011, 1654, and 3287  $\text{cm}^{-1}$ , respectively. The extract's greatest absorbance peak indicates the presence of phenol and flavonoid components. The evidence suggests that this is the cause of the metal ion's transformation into metallic nanoparticles.<sup>11</sup> When comparing the absorbance peaks of extract and SNPs, there were only minor variations in their locations and sizes. The stabilization of the SNPs was attributed to the actions of aromatic rings, germinal methyl and ether linkages, flavones, and terpenoids.<sup>18,19</sup>

*Brassica oleracea* was used to manufacture AgNPs using a green technique. *B. oleracea* AgNPs contained phenolic groups and useful proteins, as revealed by FTIR analysis, which are crucial for stabilizing the nanoparticle formation as stated by Oves et al.<sup>3</sup> Due to the study, the peaks at 1015, 1012, and 1011 are according to C–O stretching vibrations in ether, while the peaks at 1122, 1114, 1112, and 1107 are according to C–O stretching vibrations in ether and alcohol. As stated by Sriramulu and Sumathi and according to the findings, the peaks of alkane (C–H), phenol (OH), and carboxylic acid (CH) bonds will occur at 1394 and 1393  $\text{cm}^{-1}$ , respectively. According to C–C stretching vibrations in alkene, compounds are represented by the bands at 1654, 1653, 1633, and 1628.<sup>20,21</sup> C–C stretching vibrations in alkynes are represented by the bands at 2135, 2130, 2117, and 2108. CH stretching vibrations in alkane are represented by the bands at 2847, 2846, and 2834. Alaraidh et al.<sup>22</sup> reported that the AgNPs bands at 3287, 3268, 3256, and 3247 in the FTIR spectrum correspond to phenols and alcohols with hydrogen bonds. AgNPs' dispersion, shape, and size were estimated using SEM. The current investigation established that *F. desertorum* AgNPs were rounded in shape and had an average particle size of 50 nm. The nanoparticles' development suggests that they were in close proximity to one another yet were kept

stable. SEM study of AgNPs from papaya fruit extract was performed by Kalimuthu et al.,<sup>23</sup> who found that the typical particle size was about 15 nm. Similarly, they reported that created AgNP SEM study revealed that the NPs are polydisperse and range in size from 40 to 50 nm. SEM analysis of SNPs from *B. oleracea* extract revealed that the typical particle size was between 40 and 50 nm. Their finding validates our SEM study and agrees with the body of literature.

The XRD pattern was used to confirm that the particles were crystalline. AgNPs have been found to have four distinct peaks at 2 values of 38.46, 44.63, 64.81, and 77.74. The unidentified peaks are caused by contaminants in the sample, or the presence of an organic material on the surface of amorphous SNPs<sup>24</sup> confirmed our findings by measuring the AgNPs crystal diameter with the Debye–Scherrer equation. The Debye–Scherrer equation estimates that AgNPs have an average crystal size of 15 nm.

In a discovery, it was found that AgNPs from *Coriandrum sativum* exhibited cubic structures with faces centered for pure Ag ions and AgNP sizes ranging from 1 to 16 nm. Extracts rich in flavonoids protect cells by lowering oxidative stress. Many food products include phenols and polyphenols, which have potent antioxidant capabilities. The DPPH, ABTS, and  $\text{H}_2\text{O}_2$  free radicals appear to be resistant to the *F. desertorum* AgNPs. AgNPs also have the highest level of overall antioxidant and reducing power activities. The superior antioxidant activity of the AgNP was demonstrated by its lower IC<sub>50</sub> value. A free radical is DPPH. The odd electron was delocalized throughout the entire material, which allowed DPPH to stabilize as free radical molecules. A dark purple hue is produced by stable DPPH in an alcohol solution. The DPPH free radicals were reduced by the SNPs in a concentration dependent manner. Ascorbic acid and silver nanoparticle concentrations are directly

inversely proportional for scavenging DPPH radicals.<sup>25</sup> AgNPs of *F. desertorum* were tested for their antioxidant effects using the ABTS free ion scavenger test. The ABTS cationic radical scavenging effect increased along with the quantities of SNPs. The results of the current study demonstrate that AgNPs efficiently scavenge ABTS. Our results were confirmed by the authors of refs 26–28 who employed *Nothapodytes nimmoniana* to make AgNPs and used them as ABTS scavengers. In the current study, a phosphomolybdenum technique that depends on the conversion of molybdenum was used to assess the antioxidant effect of the *F. desertorum* AgNPs. The study's results, which demonstrated how effective AgNPs are as antioxidants, are laudable. Comparing AgNPs to ascorbic acid reveals that they have a significant amount of total antioxidant activity. Our results were supported by ref 28. Excessive H<sub>2</sub>O<sub>2</sub> deposition causes the generation of oxygen derived free radicals like peroxide and hydroxyl radicals in biological systems, which efficiently damage cellular membranes. The substantial inhibitory effects were found to be 73.33% for *F. desertorum* AgNPs and 85.35% for ascorbic acid at a higher dose of 250 g/mL. The results of Sudha et al. and our results were substantiated by the observation that *Lippia nodiflora* AgNPs exhibited the strongest H<sub>2</sub>O<sub>2</sub> radical scavenging activity. The concentration dependent rise in AgNPs lowering power was observed. It was claimed that AgNPs had more reduction power. AgNPs have the reducing property, so the different free radicals are scavenged by AgNPs, and the AgNPs donate electrons to the free radicals and stabilize them. Polyphenols and flavonoids induced this capacity for decrease. The findings of the current study were associated with those of Carlson et al.<sup>29</sup> The AgNPs made from plant extract were tested in the current study against a range of dangerous bacteria and showed evidence of good antibacterial action. The AgNPs demonstrated considerable antibacterial effectiveness against the bacterial strains at a dosage of 40 mg/mL.<sup>30</sup> According to research by Adebayo et al.,<sup>31</sup> *S. aureus* and *K. pneumoniae* were among the Gram-positive and Gram-negative bacteria that were strongly inhibited by AgNPs produced from whole plant extracts of *Clitoria ternatea*; AgNPs antibacterial qualities are also acknowledged by Sher et al.<sup>9</sup> This outcome is supported by the already reported research, which was accompanied by Levard et al.,<sup>32</sup> who described that the NPs interaction with lysed cells' intracellular substances caused their coagulation, and the particles were thrown out of the liquid system. The Au and Ag ions mechanism of inhibition action on micro-organisms displays that the microbe treatment by metal ions prompts loss of DNA, its capability replication, and translation, as well as other cellular enzymes and proteins that are necessary for the production of ATP (coenzyme, adenosine tri-phosphate) resulting in living-cell inactivation of Jogee et al.<sup>33</sup> It has also been assumed that metal NPs mainly affect the function of membrane-bound enzymes in the chain of respiration.<sup>34</sup>

## CONCLUSIONS

In the current study, silver ions are reduced to colloidal AgNPs via *F. desertorum* plant as a reducing and stabilizing agent. These AgNPs were then confirmed for their concentration, size, morphology, and functional groups using UV–vis analysis, XRD, SEM, and FTIR, respectively. These AgNPs also exhibit improved antioxidant and antibacterial properties. According to the results of this investigation, the green synthesized AgNPs have potential uses as free radical scavengers and antimicrobial agents. Thus, AgNPs may also aid in the development of newer,

more potent drugs. These studies suggest that the production of NPs may open a door to our numerous health issues.

## AUTHOR INFORMATION

### Corresponding Authors

**Nadia Mushtaq** – Department of Botany, University of Science and Technology, Bannu 28100 KPK, Pakistan;

Email: [nadiamushtaq@ustb.edu.pk](mailto:nadiamushtaq@ustb.edu.pk)

**Fozia Fozia** – Biochemistry Department, Khyber Medical University Institute of Medical Sciences, Kohat 26000, Pakistan; [orcid.org/0000-0002-4554-7427](https://orcid.org/0000-0002-4554-7427);

Email: [drfoziaseb@yahoo.com](mailto:drfoziaseb@yahoo.com)

### Authors

**Abida Abida** – Department of Botany, University of Science and Technology, Bannu 28100 KPK, Pakistan

**Mikhliid H. Almutairi** – Zoology Department, College of Science, King Saud University, Riyadh 11451, Saudi Arabia; [orcid.org/0000-0002-0337-6412](https://orcid.org/0000-0002-0337-6412)

**Mushtaq Ahmed** – Department of Biotechnology, University of Science and Technology, Bannu 28100 KPK, Pakistan

**Naila Sher** – Department of Biotechnology, University of Science and Technology, Bannu 28100 KPK, Pakistan

**Ijaz Ahmad** – Department of Chemistry, Kohat University of Science & Technology, Kohat 26000, Pakistan; [orcid.org/0000-0002-9139-1611](https://orcid.org/0000-0002-9139-1611)

**Bader O. Almutairi** – Zoology Department, College of Science, King Saud University, Riyadh 11451, Saudi Arabia

**Zia Ullah** – College of Professional Studies, Northeastern University, Boston 02115-5005 Massachusetts, United States

Complete contact information is available at:

<https://pubs.acs.org/10.1021/acsomega.3c04373>

### Author Contributions

Conceptualization, N.M. and M.A.; data curation, A.A.; formal analysis, A.A., M.H.A., N.M., and I.A.; funding acquisition, M.H.A. and B.O.A.; investigation, A.A.; methodology, A.A.; resources, M.A., N.S., and F.F.; software, M.A.; supervision, N.M.; validation, N.M. and F.F.; writing—original draft, A.A.; writing—review and editing, M.H.A., N.M., M.A., N.S., F.F., I.A., B.O.A., and Z.U.

### Funding

The authors extend their appreciation to the Researchers Supporting Project number (RSP2023R191), King Saud University, Riyadh, Saudi Arabia.

### Notes

The authors declare no competing financial interest. Sample of the AgNPs is available from the authors.

## REFERENCES

- (1) Oves, M.; Rauf, M. A.; Qari, H. A. Therapeutic applications of biogenic silver nanomaterial synthesized from the paper flower of bougainvillea glabra (miami, pink). *Nanomaterials* **2023**, *13*, 615.
- (2) Sher, N.; Ahmed, M.; Mushtaq, N.; Khan, R. A. Calligonum polygonoides reduced nanosilver: A new generation of nanoparticle for medical applications. *Eur. J. Integr. Med.* **2020**, *33*, 101042.
- (3) Oves, M.; Rauf, M. A.; Aslam, M.; Qari, H. A.; Sonbol, H.; Ahmad, I.; Zaman, G. S.; Saeed, M. Green synthesis of silver nanoparticles by Conocarpus Lancifolius plant extract and their antimicrobial and anticancer activities. *Saudi J. Biol. Sci.* **2022**, *29*, 460–471.
- (4) Sher, N.; Ahmed, M.; Mushtaq, N.; Khan, R. A. Synthesis of biogenic silver nanoparticles from the extract of Heliotropium

- eichwaldi L. and their effect as antioxidant, antidiabetic, and anticholinesterase. *Appl. Organomet. Chem.* **2023**, *37*, No. e6950.
- (5) Sher, N.; Alkhalifah, D. H. M.; Ahmed, M.; Mushtaq, N.; Shah, F.; Foza, F.; Khan, R. A.; Hozzein, W. N.; Aboul-Soud, M. A. Comparative Study of Antimicrobial Activity of Silver, Gold, and Silver/Gold Bimetallic Nanoparticles Synthesized by Green Approach. *Molecules* **2022**, *27*, 7895.
- (6) Gopinath, K.; Kumaraguru, S.; Bhagyaraj, K.; Mohan, S.; Venkatesh, K. S.; Esakkirajan, M.; Kaleeswaran, P.; Alharbi, N. S.; Kadaikunnan, S.; Govindarajan, M.; et al. Green synthesis of silver, gold and silver/gold bimetallic nanoparticles using the *Gloriosa superba* leaf extract and their antibacterial and antibiofilm activities. *Microb. Pathog.* **2016**, *101*, 1–11.
- (7) Brand-Williams, W.; Cuvelier, M. E.; Berset, C. Use of a free radical method to evaluate antioxidant activity. *LWT - Food Sci. Technol.* **1995**, *28*, 25–30.
- (8) Ruparelia, J. P.; Chatterjee, A. K.; Duttagupta, S. P.; Mukherji, S. Strain specificity in antimicrobial activity of silver and copper nanoparticles. *Acta Biomater.* **2008**, *4*, 707–716.
- (9) Sher, N.; Ahmed, M.; Mushtaq, N.; Khan, R. A. Enhancing antioxidant, antidiabetic, and antialzheimer performance of *Hippeastrum hybridum* (L.) using silver nanoparticles. *Appl. Organomet. Chem.* **2022**, *36*, No. e6724.
- (10) Hernandez-Gomora, A. E.; Lara-Carrillo, E.; Robles-Navarro, J. B.; Scougall-Vilchis, R. J.; Hernandez-Lopez, S.; Medina-Solis, C. E.; Morales-Luckie, R. A. Biosynthesis of Silver Nanoparticles on Orthodontic Elastomeric Modules: Evaluation of Mechanical and Antibacterial Properties. *Molecules* **2017**, *22*, 1407.
- (11) Sher, N.; Ahmed, M.; Mushtaq, N. Synthesis, optimization, and characterization of silver/gold allied bimetallic from *Hippeastrum hybridum* (L.) and their ex vivo anti-acetylcholinesterase activity in rat brain. *Appl. Organomet. Chem.* **2023**, *37*, No. e7082.
- (12) Abbasi, E.; Milani, M.; Aval, S. F.; Kouhi, M.; Akbarzadeh, A.; Nasrabadi, H. T.; Nikasa, P.; Joo, S. W.; Hanifehpour, Y.; Nejati-Koshki, K.; et al. Silver nanoparticles: Synthesis methods, bio-applications and properties. *Crit. Rev. Microbiol.* **2016**, *42*, 173–180.
- (13) Ahmed, E.; Arshad, M.; Ahmad, M.; Saeed, M.; Ishaque, M. Ethnopharmacological survey of some medicinally important plants of Galliyat Areas of NWFP, Pakistan. *Asian J. Plant Sci.* **2004**, *3*, 410–415.
- (14) Ahmed, S.; Ahmad, M.; Swami, B. L.; Ikram, S. A review on plants extract mediated synthesis of silver nanoparticles for antimicrobial applications: A green expertise. *J. Adv. Res.* **2016**, *7*, 17–28.
- (15) Ramkumar, V. S.; Pugazhendhi, A.; Prakash, S.; Ahila, N. K.; Vinoj, G.; Selvam, S.; Kumar, G.; Kannapiran, E.; Rajendran, R. B. Synthesis of platinum nanoparticles using seaweed *Padina gymnospora* and their catalytic activity as PVP/PtNPs nanocomposite towards biological applications. *Biomed. Pharmacother.* **2017**, *92*, 479–490.
- (16) Kumar, G. A.; Bodke, Y. D.; Manjunatha, B.; Satyanarayan, N.; Nippu, B.; Muthipeedika, N. J. Novel synthesis of 3-(Phenyl)-(ethylamino methyl)-4-hydroxy-2H-chromen-2-one derivatives using biogenic ZnO nanoparticles and their applications. *Chim. Techno Acta* **2022**, *9*, 20229104.
- (17) Hazarika, D.; Phukan, A.; Saikia, E.; Chetia, B. Phytochemical screening and synthesis of silver nanoparticles using leaf extract of *Rhynchosyche ellipticum*. *Int. J. Pharm. Pharm. Sci.* **2014**, *6*, 672–674.
- (18) Ahmad, A.; Syed, F.; Shah, A.; Khan, Z.; Tahir, K.; Khan, A. U.; Yuan, Q. Silver and gold nanoparticles from *Sargentodoxa cuneata*: synthesis, characterization and antileishmanial activity. *RSC Adv.* **2015**, *5*, 73793–73806.
- (19) Ahmed, H. B.; Attia, M. A.; El-Dars, F.; Emam, H. E. Hydroxyethyl cellulose for spontaneous synthesis of antipathogenic nanostructures: (Ag & Au) nanoparticles versus Ag-Au nano-alloy. *Int. J. Biol. Macromol.* **2019**, *128*, 214–229.
- (20) Syed, B.; Bisht, N.; Prithvi, S. B.; Karthik, R. N.; Prasad, A.; Dhananjaya, B. L.; Satish, S.; Prasad, H.; Prasad, M. N. N. Phytogenic synthesis of nanoparticles from *Rhizophora mangle* and their bactericidal potential with DNA damage activity. *Nano-Struct. Nano-Objects* **2017**, *10*, 112–115.
- (21) Awwad, A. M.; Salem, N. M.; Abdeen, A. O. Green synthesis of silver nanoparticles using carob leaf extract and its antibacterial activity. *Int. J. Ind. Chem.* **2013**, *4*, 29.
- (22) Alaraidh, I. A.; Ibrahim, M. M.; El-Gaaly, G. A. Evaluation of Green Synthesis of Ag Nanoparticles Using *Eruca sativa* and *Spinacia oleracea* Leaf Extracts and Their Antimicrobial Activity. *J. Nanomater.* **2014**, *12*, 50–55.
- (23) Kalimuthu, K.; Babu, R. S.; Venkataraman, D.; Bilal, M.; Gurunathan, S. Biosynthesis of silver nanocrystals by *Bacillus licheniformis*. *Colloids Surf., B* **2008**, *65*, 150–153.
- (24) Ruddaraju, L. K.; Pallela, P. N. V. K.; Pammi, S. V. N.; Padavala, V. S.; Kolapalli, V. R. M. Synergistic antibacterial and anticarcinogenic effects of *Annona squamosa* leaf extract mediated silver nano particles. *Mater. Sci. Semicond. Process.* **2019**, *100*, 301–309.
- (25) Gahlawat, G.; Shikha, S.; Chaddha, B. S.; Chaudhuri, S. R.; Mayilraj, S.; Choudhury, A. R. Microbial glycolipoprotein-capped silver nanoparticles as emerging antibacterial agents against cholera. *Microb. Cell Fact.* **2016**, *15*, 25.
- (26) Suriyakala, G.; Sathiyaraj, S.; Devanesan, S.; AlSalhi, M. S.; Rajasekar, A.; Maruthamuthu, M. K.; Babujanathanam, R. Phytosynthesis of silver nanoparticles from *Jatropha integerrima* Jacq. flower extract and their possible applications as antibacterial and antioxidant agent. *Saudi J. Biol. Sci.* **2022**, *29*, 680–688.
- (27) Sathiyaraj, S.; Suriyakala, G.; Dhanesh Gandhi, A.; Babujanathanam, R.; Almaary, K. S.; Chen, T.; Kaviyarasu, K. Biosynthesis, characterization, and antibacterial activity of gold nanoparticles. *J. Infect. Public Health* **2021**, *14*, 1842–1847.
- (28) Gandhi, A. D.; Kaviyarasu, K.; Supraja, N.; Velmurugan, R.; Suriyakala, G.; Babujanathanam, R.; Zang, Y.; Soontarapa, K.; Almaary, K. S.; Elshikh, M. S.; et al. Annealing dependent synthesis of cyto-compatible nano-silver/calcium hydroxyapatite composite for antimicrobial activities. *Arabian J. Chem.* **2021**, *14*, 103404.
- (29) Carlson, C.; Hussain, S. M.; Schrand, A. M.; Braydich-Stolle, L. K.; Hess, K. L.; Jones, R. L.; Schlager, J. J. Unique cellular interaction of silver nanoparticles: size-dependent generation of reactive oxygen species. *J. Phys. Chem. B* **2008**, *112*, 13608–13619.
- (30) Abdul, R. P.; Abbas, Q.; Ali, A.; Raza, H.; Kim, S. J.; Zia, M.; Haq, I. Antioxidant, cytotoxic and antimicrobial activities of green synthesized silver nanoparticles from crude extract of *Bergenia ciliata*. *Future J. Pharm. Sci.* **2016**, *2*, 31–36.
- (31) Adebayo, E. A.; Ibikunle, J. B.; Oke, A. M.; Lateef, A.; Azeez, M. A.; Oluwatoyin, A. O.; AyanfeOluwa, A. V.; Blessing, O. T.; Comfort, O. O.; Adekunle, O. O. Antimicrobial and antioxidant activity of silver, gold and silver-gold alloy nanoparticles phytosynthesized using extract of *Opuntia ficus-indica*. *J. Rev. Adv. Mater. Sci.* **2019**, *58*, 313–326.
- (32) Levard, C.; Hotze, E. M.; Lowry, G. V.; Brown, G. E., Jr. Environmental transformations of silver nanoparticles: impact on stability and toxicity. *Environ. Sci. Technol.* **2012**, *46*, 6900–6914.
- (33) Joo, P. S.; Ingle, A. P.; Rai, M. Isolation and identification of toxigenic fungi from infected peanuts and efficacy of silver nanoparticles against them. *Food Control* **2017**, *71*, 143–151. From <http://worldcat.org/z-wcorg/>.
- (34) Fakhri, A.; Tahami, S.; Naji, M. Synthesis and characterization of core-shell bimetallic nanoparticles for synergistic antimicrobial effect studies in combination with doxycycline on burn specific pathogens. *J. Photochem. Photobiol., B* **2017**, *169*, 21–26.